Supplemental Figure S2

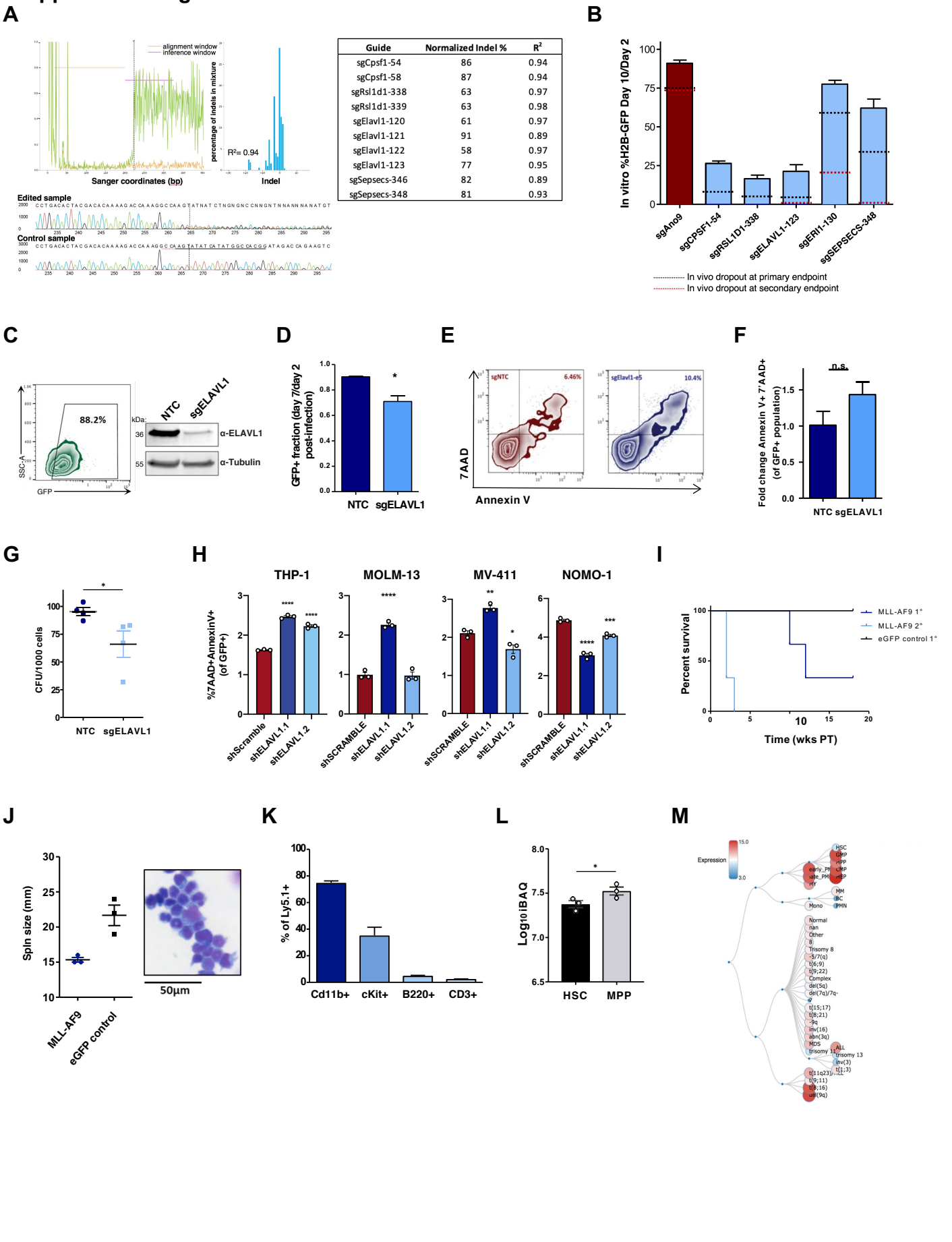

Supplemental Figure S2. Validation and characterization of primary and secondary screen hit-targeting sgRNAs. (A) Representative indel plots and traces generated from ICE analysis41 for individually validated sgRNAs in test RN2c cells. Level of discordance (top left) in the sample sequence (green) and control sequence (orange) before and after the expected cut-site is shown. Indel plot (top right) shows percentages of the various calculated indel sizes. Trace sequences (bottom) display the aligned sample and control sequences with the targeted cut-site. Indel percentages for individually validated sgRNAs normalized to the percent infection of each sample. R2 values were generated from Indel plots. (B) *In vitro* assessment of RN2c growth upon knockout of selected screen hits. Levels of H2B-GFP reduction achieved in parallel *in vivo* experiments in primary and secondary mice are highlighted in black and red dotted lines respectively. (C) Western blot validation of ELAVL1 knockout by pL.CRISPR.EFS.GFP-sgELAVL1 in HEK293 cells one week post-infection. Prior to lysis, cultures were analyzed by flow cytometry for the fraction of GFP+ cells; sgNTC was used as a negative control. (D) sgRNA-mediated KO of ELAVL1 in THP-1 cells; GFP+ fraction was followed over time. GFP+ fractions of sgNTC and sgELAVL1 infected THP-1 cells at 7 days post-transduction are normalized to the percent infected at 2 days PT. (E,F) Representative flow plots (E) and quantitative analysis of the apoptotic fraction of GFP+ shScramble and shELAVL1 THP-1 cells 4 days post-plating (F). Data represents 3 replicate infections. (G) CFU assays performed with FACS-purified GFP+ sgNTC and sgELAVL1 THP-1 cells. (H) Cell death quantified by flow cytometric analysis in AML cell lines (THP-1, MOLM-13, MV-411, NOMO-1) 4 days post-infection with shRNA targeting ELAVL1 and Scramble (control).

(I) B6.SJL mouse LSK cells were retrovirally infected with MSCV-MLLAF9-PGK-eGFP (or MSCV-PGK-eGFP, control) and GFP+ cells FACS-purified 48hr post-infection transplanted into C57Blk/6 recipients. Fully engrafted primary MLL-AF9-driven leukemic BM was challenged in secondary recipients. Latency of primary (1°) and secondary (2°) transplant MLL-AF9 leukemias, as well as primary eGFP control BM (n = 3 for each arm) is shown. (J) Spleen sizes of primary engrafted MLL-AF9-driven leukemias and primary eGFP control BM (left) and Wright-Giemsa staining of peripheral blood sampled from primary engrafted recipient mouse in MLL-AF9 arm (right). (K) Flow cytometric evaluation of the immunophenotype of MLL-AF9-driven BM grafts.

(L) Expression levels of Elavl1 in mouse HSC (LSK CD34-CD150+CD48-FLK2-) and MPP (LSK CD34+CD15-+CD48-FLK2-) populations42. Intensity based absolute quantification (iBAQ) levels are shown. (M) Correlation tree of normal and malignant hematopoietic samples based on *ELAVL1* expression levels generated by the BloodPool tool, adapted from Bloodspot43 showcasing low (blue) expression in HSCs relative to higher (pink to red) expression in bulk AML cells.